

# Nuclear medium effects in Drell-Yan process

H. Haider,<sup>1</sup> M. Sajjad Athar,<sup>1,\*</sup> S. K. Singh,<sup>1</sup> and I. Ruiz Simo<sup>2</sup>

<sup>1</sup>*Department of Physics, Aligarh Muslim University, Aligarh - 202 002, India*

<sup>2</sup>*Departamento de Física Atómica, Molecular y Nuclear,*

*and Instituto de Física Teórica y Computacional Carlos I, Universidad de Granada, Granada 18071, Spain*

We study nuclear medium effects in Drell-Yan processes using quark parton distribution functions in a microscopic nuclear model which takes into account the effect of Fermi motion, nuclear binding and nucleon correlations through a relativistic nucleon spectral function. The contributions of  $\pi$  and  $\rho$  mesons are also included. The beam energy loss is calculated assuming forward propagation of beam partons using Eikonal approximation. The results are compared with the theoretical and experimental results. The model is able to successfully explain the low target  $x_t$  results of E772 and E866 Drell-Yan experiments and is applicable to the forthcoming experimental analysis of E906 Sea Quest experiment at Fermi Lab.

PACS numbers: 13.40.-f, 21.65.-f, 24.85.+p, 25.40.-h

## I. INTRODUCTION

Drell-Yan production of lepton pairs [1] from nucleons and nuclear targets is an important tool to study the quark structure of nucleons and its modification in the nuclear medium. In particular, the proton induced Drell-Yan production of muon pairs on nucleons and nuclei provides a direct probe to investigate the quark parton distribution functions (PDFs). The Drell-Yan (DY) production takes place through basic process of quark-antiquark annihilation into lepton pairs i.e.  $q^{b(t)} + \bar{q}^{t(b)} \rightarrow l^+ + l^-$  where b and t indicate the beam proton and the target nucleon. In this basic process a quark (antiquark) in the beam carrying a longitudinal momentum fraction  $x_b$  interacts with an antiquark (quark) in the target carrying longitudinal momentum fraction  $x_t$  of the target momentum per nucleon to produce a virtual photon which decays into lepton pairs.

The cross section per target nucleon  $\frac{d^2\sigma}{dx_b dx_t}$  in the leading order is given by [2]:

$$\frac{d^2\sigma}{dx_b dx_t} = \frac{4\pi\alpha^2}{9Q^2} \sum_f e_f^2 \{q_f^b(x_b, Q^2)\bar{q}_f^t(x_t, Q^2) + \bar{q}_f^b(x_b, Q^2)q_f^t(x_t, Q^2)\} \quad (1)$$

where  $\alpha$  is the fine structure constant,  $e_f$  is the charge of quark (antiquark) of flavor f,  $Q^2$  is the photon virtuality and  $q_f^{b,t}(x)$  and  $\bar{q}_f^{b,t}(x)$  are the beam (target) quark/antiquark PDFs.

This process is directly sensitive to the antiquark parton distribution functions  $\bar{q}(x)$  in target nuclei which has also been studied by DIS experiments through the observation of EMC effect. Quantitatively the EMC effect describes the nuclear modification of nucleon structure function  $F_2(x_t)$  for the bound nucleon defined as  $F_2(x_t) = x_t \sum_f e_f^2 [q_f(x_t) + \bar{q}_f(x_t)]$  and gives information about the modification of the sum of quark and antiquark PDFs [3, 4] which is dominated by the valence quarks in the high  $x_t$  region ( $x_t > 0.3$ ). In the low  $x_t$  region ( $x_t \leq 0.3$ ), where sea quarks are expected to give dominant contribution, the study of  $F_2(x)$  gives information about sea quark and antiquark PDFs. Thus, nuclear modifications are phenomenologically incorporated in  $q(x_t)$  and  $\bar{q}(x_t)$  using the experimental data on  $F_2(x_t)$  and are used to analyze the DY yields from nuclear targets. Some authors succeed in giving a satisfactory description of DIS and DY data on nuclear targets using same set of nuclear  $q(x)$  and  $\bar{q}(x)$  [5], while some others find it difficult to provide a consistent description of DIS and DY data using the same set of nuclear PDFs [6]. On the other hand, there are many theoretical attempts to describe the nuclear modifications of quark and antiquark PDFs to explain DIS which have been used to describe the DY process on nuclear targets [7]-[21]. The known nuclear modifications discussed in literature in the case of DIS are (a) modification of nucleon structure inside the nuclear medium, (b) a significantly enhanced contribution of subnucleonic degrees of freedom like pions or quark clusters in nuclei and (c) nuclear shadowing.

However, in the case of DY processes there is an additional nuclear effect due to initial state interaction of beam partons with the target partons which may be present before the hard collisions of these partons produce lepton pairs.

---

\*Electronic address: sajjathar@gmail.com

As the initial beam traverses the nuclear medium it loses energy due to interaction of beam partons with nuclear constituents of the target. This can be visualized in terms of the interaction of hadrons or its constituents with the constituents of the target nucleus through various inelastic processes leading to energy loss of the interacting beam partons. This has been studied phenomenologically using available parameterization of nuclear PDFs or theoretically in models based on QCD or Glauber approaches taking into account the effect of shadowing which also plays an important role in the low  $x_t$  region but any consensus in the understanding of physics behind the beam energy loss has been lacking [22–26]. This is also the region in which modification of sea quark PDF due to mesonic contributions are also important. It is however known that mesonic contributions enhance DY yields (and  $F_2(x)$  in DIS) while the shadowing and parton energy loss effects suppress them. Since, we are not studying the shadowing effect here in this work, therefore, we confine ourselves to the region of  $x_t > 0.1$ , where shadowing does not play a major role. In this region, the main nuclear effects are the mesonic contributions and nuclear structure effects as in the case of DIS with additional effect of parton energy loss in the beam parton energy due to the presence of nuclear targets.

In this paper, we present the results of nuclear medium effects on DY production of lepton pairs calculated in a theoretical microscopic nuclear model which has been successfully used to describe the DIS of charged leptons and  $\nu(\bar{\nu})$  from various nuclei [27–32]. The model uses a relativistic nucleon spectral function to describe target nucleon momentum distribution incorporating Fermi motion, binding energy effects and nucleon correlations in a field theoretical model. The model has also been used to include the mesonic contributions from  $\pi$  and  $\rho$  mesons. The beam energy loss has been calculated in a model where the incoming beam proton loses energy in inelastic collisions with the target hadrons as it travels the nuclear medium. This has been parameterized in terms of proton-nucleon scattering cross section using Glauber approach [21]. The results have been presented for the kinematic region of experiments E772 [33] and E866 [26, 34] for proton induced DY processes in nuclear targets like  ${}^9\text{Be}$ ,  ${}^{12}\text{C}$ ,  ${}^{40}\text{Ca}$ ,  ${}^{56}\text{Fe}$  and  ${}^{184}\text{W}$  in the region of  $x_t > 0.1$ . The numerical results extended up to  $x_t = 0.45$ , should be useful in analyzing the forthcoming experimental results from the SeaQuest E906 experiment being done at Fermi Lab [35].

In section-II, we present the formalism in brief, in section III, the results are presented and discussed and finally in section IV we summarize the results and conclude our findings.

## II. NUCLEAR EFFECTS

When DY processes take place in nuclei, nuclear effects appear which are generally believed to be due to

- (a) nuclear structure arising from Fermi motion, binding energy and nucleon correlations
- (b) additional contribution due to subnucleonic degrees of freedom like mesons and/or quark cluster in the nuclei and
- (c) energy loss of the beam proton as it traverses the nuclear medium before producing lepton pairs.

In the case of proton induced DY processes in nuclei, the target nucleon has a Fermi momentum described by a momentum distribution. The target Bjorken variable  $x_t$ , defined for a free nucleon which is expressed covariantly as  $x_t = \frac{2q \cdot p_1}{(p_1 + p_2)^2}$ , where  $q$  is the four momentum of  $\mu^+\mu^-$  pair,  $p_{1\mu}$  and  $p_{2\mu}$  are beam and target four momenta has a Fermi momentum dependence in the nuclear medium. Moreover, the projectile Bjorken variable  $x_b$  expressed covariantly as  $x_b = \frac{2q \cdot p_2}{(p_1 + p_2)^2}$  also changes due to the energy loss of the beam particle caused by the initial state interactions with the nuclear constituents as it travels through the nuclear medium before producing lepton pairs. These nuclear modifications in  $x_b$  and  $x_t$  are incorporated while evaluating Eq. 1. Furthermore, there are additional contributions from the pion and rho mesons which are also taken into account.

In the following, we briefly outline the model and refer to earlier work [21, 27–32] for details.

### A. Nuclear Structure

In a nucleus, scattering is assumed to take place from partons inside the individual nucleons which are bound in the nucleus and moving with a Fermi momentum  $\vec{p}$ . The target Bjorken variable  $x_t$  becomes Fermi momentum dependent and PDF for quarks and antiquarks in the nucleus i.e.  $q_f^i(x_t)$  and  $\bar{q}_f^i(x_t)$  are calculated as a convolution of the PDFs in bound nucleon and a momentum distribution function of the nucleon inside the nucleus. The parameters of the momentum distribution are adjusted to correctly incorporate nuclear properties like binding energy, Fermi motion and the nucleon correlation effects in the nuclear medium. We use the Lehmann representation of the relativistic Dirac propagator for an interacting Fermi sea in nuclear matter to derive such a momentum distribution and use Local Density Approximation to translate at a position  $\mathbf{r}$  in the nucleus to describe the finite nucleus [21, 29–32]. The relativistic propagator for a nucleon of mass  $M_N$  is written in terms of positive and negative energy components as

$$G^0(p_0, \mathbf{p}) = \frac{M_N}{E(\mathbf{p})} \left\{ \frac{\sum_r u_r(p) \bar{u}_r(p)}{p^0 - E(\mathbf{p}) + i\epsilon} + \frac{\sum_r v_r(-p) \bar{v}_r(-p)}{p^0 + E(\mathbf{p}) - i\epsilon} \right\} \quad (2)$$

For a noninteracting Fermi sea where only positive energy solutions are considered the relevant propagator is rewritten in terms of occupation number  $n(\mathbf{p}) = 1$  for  $p \leq p_F$  while  $n(\mathbf{p})=0$  for  $p > p_F$ :

$$G^0(p_0, \mathbf{p}) = \frac{M_N}{E(\mathbf{p})} \left\{ \sum_r u_r(p) \bar{u}_r(p) \left[ \frac{1 - n(p)}{p^0 - E(\mathbf{p}) + i\epsilon} + \frac{n(p)}{p^0 - E(\mathbf{p}) - i\epsilon} \right] \right\} \quad (3)$$

The nucleon propagator for a nucleon in an interacting Fermi sea is then calculated by making a perturbative expansion of  $G(p_0, \mathbf{p})$  in terms of  $G^0(p_0, \mathbf{p})$  given in equation(2) by retaining the positive energy contributions only (the negative energy components are suppressed).

This perturbative expansion is then summed in ladder approximation to give [27, 36]

$$\begin{aligned} G(p_0, \mathbf{p}) &= \frac{M_N}{E(\mathbf{p})} \sum_r u_r(p) \bar{u}_r(p) \frac{1}{p^0 - E(\mathbf{p})} + \frac{M_N}{E(\mathbf{p})} \sum_r \frac{u_r(p) \bar{u}_r(p)}{p^0 - E(\mathbf{p})} \sum(p^0, \mathbf{p}) \frac{M_N}{E(\mathbf{p})} \sum_s \frac{u_s(p) \bar{u}_s(p)}{p^0 - E(\mathbf{p})} + \dots \quad (4) \\ &= \frac{M_N}{E(\mathbf{p})} \sum_r \frac{u_r(p) \bar{u}_r(p)}{p^0 - E(\mathbf{p}) - \bar{u}_r(p) \sum(p^0, \mathbf{p}) u_r(p) \frac{M_N}{E(\mathbf{p})}}, \end{aligned}$$

where  $\sum(p^0, \mathbf{p})$  is the nucleon self energy.

This allows us to write the relativistic nucleon propagator in a nuclear medium in terms of the Spectral functions of holes and particles as [36]

$$G(p^0, \mathbf{p}) = \frac{M_N}{E(\mathbf{p})} \sum_r u_r(\mathbf{p}) \bar{u}_r(\mathbf{p}) \left[ \int_{-\infty}^{\mu} d\omega \frac{S_h(\omega, \mathbf{p})}{p^0 - \omega - i\eta} + \int_{\mu}^{\infty} d\omega \frac{S_p(\omega, \mathbf{p})}{p^0 - \omega + i\eta} \right] \quad (5)$$

$S_h(\omega, \mathbf{p})$  and  $S_p(\omega, \mathbf{p})$  being the hole and particle spectral functions respectively, which are derived in Ref. [36]. We use:

$$S_h(p^0, \mathbf{p}) = \frac{1}{\pi} \frac{\frac{M_N}{E(\mathbf{p})} \text{Im} \Sigma^N(p^0, \mathbf{p})}{(p^0 - E(\mathbf{p}) - \frac{M_N}{E(\mathbf{p})} \text{Re} \Sigma^N(p^0, \mathbf{p}))^2 + (\frac{M_N}{E(\mathbf{p})} \text{Im} \Sigma^N(p^0, \mathbf{p}))^2} \quad (6)$$

for  $p^0 \leq \mu$

$$S_p(p^0, \mathbf{p}) = -\frac{1}{\pi} \frac{\frac{M_N}{E(\mathbf{p})} \text{Im} \Sigma^N(p^0, \mathbf{p})}{(p^0 - E(\mathbf{p}) - \frac{M_N}{E(\mathbf{p})} \text{Re} \Sigma^N(p^0, \mathbf{p}))^2 + (\frac{M_N}{E(\mathbf{p})} \text{Im} \Sigma^N(p^0, \mathbf{p}))^2} \quad (7)$$

for  $p^0 > \mu$ .

The normalization of this spectral function is obtained by imposing the baryon number conservation following the method of Frankfurt and Strikman [37]. In the present paper, we use local density approximation (LDA) where we do not have a box of constant density, and the reaction takes place at a point  $\mathbf{r}$ , lying inside a volume element  $d^3r$  with local density  $\rho_p(\mathbf{r})$  and  $\rho_n(\mathbf{r})$  corresponding to the proton and neutron densities at the point  $\mathbf{r}$ . This leads to the spectral functions for the protons and neutrons to be the function of local Fermi momentum given by

$$k_{F_p}(\mathbf{r}) = [3\pi^2 \rho_p(\mathbf{r})]^{1/3}, \quad k_{F_n}(\mathbf{r}) = [3\pi^2 \rho_n(\mathbf{r})]^{1/3} \quad (8)$$

and therefore the normalization condition may be imposed as

$$2 \int \frac{d^3p}{(2\pi)^3} \int_{-\infty}^{\mu} S_h^{p(n)}(\omega, \mathbf{p}, k_{F_{p,n}}(\mathbf{r})) d\omega = \rho_{p,n}(\mathbf{r}) \quad (9)$$

leading to the normalization condition given by

$$2 \int d^3r \int \frac{d^3p}{(2\pi)^3} \int_{-\infty}^{\mu} S_h^{p(n)}(\omega, \mathbf{p}, \rho_{p(n)}(\mathbf{r})) d\omega = Z(N), \quad (10)$$

where  $\rho(r)$  is the baryon density for the nucleus which is normalized to A and is taken from the electron nucleus scattering experiments. The average kinetic and total nucleon energy in a nucleus with the same number of protons and neutrons are given by:

$$\langle T \rangle = \frac{4}{A} \int d^3r \int \frac{d^3p}{(2\pi)^3} (E(\mathbf{p}) - M_N) \int_{-\infty}^{\mu} S_h(p^0, \mathbf{p}, \rho(r)) dp^0, \quad (11)$$

$$\langle E \rangle = \frac{4}{A} \int d^3r \int \frac{d^3p}{(2\pi)^3} \int_{-\infty}^{\mu} S_h(p^0, \mathbf{p}, \rho(r)) p^0 dp^0, \quad (12)$$

and the binding energy per nucleon is given by [27]:

$$|E_A| = -\frac{1}{2}(\langle E - M_N \rangle + \frac{A-2}{A-1} \langle T \rangle) \quad (13)$$

The binding energy per nucleon for each nucleus is correctly reproduced to match with the experimentally observed values. This spectral function has been used to describe the DIS of charged leptons on the nuclear targets. In the case of nucleus, the nuclear hadronic tensor  $W_A^{\mu\nu}$  for an isospin symmetric nucleus is derived to be [27, 29]:

$$W_A^{\mu\nu} = 2 \sum_{i=p,n} \int d^3r \int \frac{d^3p}{(2\pi)^3} \frac{M_N}{E(\vec{p})} \int_{-\infty}^{\mu} dp^0 S_h(p^0, \mathbf{p}, \rho_i) W_i^{\mu\nu}(p, q) \quad (14)$$

where the factor 2 is a spin factor and using this the electromagnetic structure function  $F_{2A}(x, Q^2)$  for a non-symmetric ( $N \neq Z$ ) nucleus in DIS is obtained as [27],

$$F_{2A}^t(x, Q^2) = 2 \sum_{i=p,n} \int d^3r \int \frac{d^3p}{(2\pi)^3} \frac{M_N}{E(\mathbf{p})} \int_{-\infty}^{\mu_i} dp^0 S_h^i(p^0, \mathbf{p}, \rho_i(r)) \sum_f e_f^2 x_t' [q_f^i(x_t'(p^0, \vec{p})) + \bar{q}_f^i(x_t'(p^0, \vec{p}))] \quad (15)$$

For the numerical calculations, we have used CTEQ6.6 [38] nucleon parton distribution functions(PDFs) for  $q_f^i$  and  $\bar{q}_f^i$ .  $S_h^i$  are the two different spectral functions, each of them normalized to the number of protons or neutrons in the nuclear target.  $\rho_p(\rho_n)$  is the proton(neutron) density inside the nucleus.

We see that the nuclear structure effects like Fermi motion, binding energy and nucleon correlations are properly incorporated for bound quarks in nucleons in a nucleus and we write  $q_f^t(x_t)$  as [21]:

$$\begin{aligned} q_f^t(x_t, Q^2) &= 2 \sum_{i=p,n} \int d^3r \int \frac{d^3p}{(2\pi)^3} \frac{M_N}{E(\mathbf{p})} \int_{-\infty}^{\mu_i} dp^0 S_h^i(p^0, \mathbf{p}, \rho_i(r)) q_f^i(x_t'(p^0, \vec{p}), Q^2) \\ \bar{q}_f^t(x_t, Q^2) &= 2 \sum_{i=p,n} \int d^3r \int \frac{d^3p}{(2\pi)^3} \frac{M_N}{E(\mathbf{p})} \int_{-\infty}^{\mu_i} dp^0 S_h^i(p^0, \mathbf{p}, \rho_i(r)) \bar{q}_f^i(x_t'(p^0, \vec{p}), Q^2), \end{aligned} \quad (16)$$

where  $q_f^i(\bar{q}_f^i(x_t, Q^2))$  is the quark(antiquark) PDFs for flavor f inside a nucleon and the factor of 2 is because of quark(antiquark) spin degrees of freedom.  $x_t' = \frac{M_N}{p^0 - p_z} x_t$  which is obtained from the covariant expression of  $x_t' = \frac{q \cdot p_1}{s_N}$  with  $\vec{p}_1 \parallel z$  direction.

## B. Mesonic contributions

Mesonic contributions are taken into account by making use of the imaginary part of the meson propagators instead of spectral function which were derived from the imaginary part of the propagator in the case of nucleon. So in the case of pion, we replace in Eq.(15) [29]

$$\frac{M_N}{E(\mathbf{p})} \int_{-\infty}^{\mu} d\omega S_h(\omega, \mathbf{p}) \delta(p^0 - \omega) \rightarrow -\frac{1}{\pi} \theta(p_0) \text{Im}D(p)$$

where  $D(p)$  is the pion propagator in the nuclear medium given by

$$D(p) = [p^{02} - \vec{p}^2 - m_\pi^2 - \Pi_\pi(p^0, \mathbf{p})]^{-1}, \quad (17)$$

where

$$\Pi_\pi = \frac{f^2/m_\pi^2 F^2(p) \vec{p}^2 \Pi^*}{1 - f^2/m_\pi^2 V_L' \Pi^*}. \quad (18)$$

Here,  $F(p) = (\Lambda^2 - m_\pi^2)/(\Lambda^2 + \vec{p}^2)$  is the  $\pi NN$  form factor,  $\Lambda = 1\text{GeV}$ ,  $f = 1.01$ ,  $V_L'$  is the longitudinal part of the spin-isospin interaction and  $\Pi^*$  is the irreducible pion self energy that contains the contribution of particle - hole and delta - hole excitations.

Following a similar procedure, as done in the case of nucleon, the contribution of the pions to hadronic tensor in the nuclear medium may be written as [27]

$$W_{A,\pi}^{\mu\nu} = 3 \int d^3r \int \frac{d^4p}{(2\pi)^4} \theta(p^0) (-2) \text{Im}D(p) 2m_\pi W_\pi^{\mu\nu}(p, q) \quad (19)$$

However, Eq.(19) also contains the contribution of the pionic contents of the nucleon, which are already contained in the sea contribution of nucleon through Eq.(16), therefore, the pionic contribution of the nucleon is to be subtracted from Eq.(19), in order to calculate the contribution from the excess pions in the nuclear medium. This is obtained by replacing  $\text{Im}D(p)$  by  $\delta\text{Im}D(p)$  [27] as

$$\text{Im}D(p) \rightarrow \delta\text{Im}D(p) \equiv \text{Im}D(p) - \rho \frac{\partial \text{Im}D(p)}{\partial \rho} \Big|_{\rho=0} \quad (20)$$

Using Eq.19, pion structure function  $F_{2,\pi}^A(x_A)$  in a nucleus is derived as

$$F_{2,\pi}^A(x) = -6 \int d^3r \int \frac{d^4p}{(2\pi)^4} \theta(p^0) \delta\text{Im}D(p) \frac{x}{x_\pi} 2M_N \sum_f e_f^2 x_\pi [q_\pi^f(x_\pi(p^0, \vec{p})) + \bar{q}_\pi^f(x_\pi(p^0, \vec{p}))] \theta(x_\pi - x) \theta(1 - x_\pi), \quad (21)$$

where  $\frac{x}{x_\pi} = \frac{-p^0 + p^z}{M_N}$ .

Following a similar procedure, as done in the case of nucleon, the expression for the pion quark PDF in the nuclear medium  $q_{f,\pi}^t(x_t, Q^2)$  is derived as [21]:

$$q_{f,\pi}^t(x_t, Q^2) = -6 \int d^3r \int \frac{d^4p}{(2\pi)^4} \theta(p^0) \delta\text{Im}D_\pi(p) 2M_N q_{f,\pi}(x_\pi) \theta(x_\pi - x_t) \theta(1 - x_\pi). \quad (22)$$

and a similar expression for  $\bar{q}_{f,\pi}^t(x_t, Q^2)$ .

Similarly the contribution of the  $\rho$ -meson cloud to the structure function is taken into account in analogy with the above prescription and the rho structure function is written as [27]

$$F_{2,\rho}^A(x) = -12 \int d^3r \int \frac{d^4p}{(2\pi)^4} \theta(p^0) \delta\text{Im}D_\rho(p) \frac{x}{x_\rho} 2M_N \sum_f e_f^2 x_\rho [q_\rho^f(x_\rho(p^0, \vec{p})) + \bar{q}_\rho^f(x_\rho(p^0, \vec{p}))] \theta(1 - x_\rho) \theta(x_\rho - x) \quad (23)$$

and the expression for the rho PDF  $q_{f,\rho}^t(x_t, Q^2)$  is derived as [21]:

$$q_{f,\rho}^t(x_t, Q^2) = -12 \int d^3r \int \frac{d^4p}{(2\pi)^4} \theta(p^0) \delta\text{Im}D_\rho(p) 2M_N q_{f,\rho}(x_\rho) \theta(x_\rho - x_t) \theta(1 - x_\rho), \quad (24)$$

where  $D_\rho(p)$  is now the  $\rho$ -meson propagator in the medium given by:

$$D_\rho(p) = [p^0{}^2 - \vec{p}^2 - m_\pi^2 - \Pi_\rho^*(p^0, \mathbf{p})]^{-1}, \quad (25)$$

where

$$\Pi_\rho^* = \frac{f^2/m_\rho^2 C_\rho F_\rho^2(p) \vec{p}^2 \Pi^*}{1 - f^2/m_\rho^2 V_T' \Pi^*}. \quad (26)$$

Here,  $V_T'$  is the transverse part of the spin-isospin interaction,  $C_\rho = 3.94$ ,  $F_\rho(p) = (\Lambda_\rho^2 - m_\rho^2)/(\Lambda_\rho^2 + \vec{p}^2)$  is the  $\rho NN$  form factor,  $\Lambda_\rho = 1\text{GeV}$ ,  $f = 1.01$ , and  $\Pi^*$  is the irreducible rho self energy that contains the contribution of particle - hole and delta - hole excitations,  $\frac{x}{x_\rho} = \frac{-p^0 + p^z}{M_N}$ . Quark and antiquark PDFs for pions have been taken from the parameterization given by Gluck et al. Ref.[39] and for the rho mesons we have taken the same PDFs as for the pions.

### C. Energy loss of beam partons

The incident proton beam traverses the nuclear medium before the beam parton undergoes a hard collision with the target parton. The incident proton may lose energy due to soft inelastic collisions, it might scatter on its way within the nucleus before producing a lepton pair. We shall consider the region  $x_t > 0.1$  (away from the shadowing

region), and assume that the initial state interactions are manifested through the inelastic proton-proton collisions in the case of proton induced DY processes from nuclei. We further assume that each collision of this type occurs with a probability  $\sigma_{NN}\rho dl$  during a length of  $l$  in the nuclear medium with nuclear density  $\rho$ , the proton loses a fraction  $\beta$  of its energy. In principle,  $\beta$  may depend upon energy but we assume it to be constant. With this assumption, the energy  $E_b$  of the beam parton is described by [21]:

$$\begin{aligned}\frac{dE_b}{dl} &= -\sigma_{NN}\rho\beta E_b \\ E_b(\vec{r}) &= E_{b\text{ in}} \exp[-\beta\sigma_{NN} \int_{-\infty}^z \rho(\vec{b}, z') dz']\end{aligned}\quad (27)$$

Since  $x_b$  is inversely proportional to  $E_b$ , we write

$$x_b(\vec{r}) = x_b \exp[\beta\sigma_{NN} \int_{-\infty}^z \rho(\vec{b}, z') dz'] \quad (28)$$

where  $\sigma_{NN}$  is the  $NN$  total cross section, ( $\sigma_{NN}$ ) taken to be 40mb [40],  $\rho(\vec{r})$  the nuclear density and  $\vec{b}$  the impact parameter.

Using these modified values of  $x_b(\mathbf{r})$ , the DY cross sections are written as

$$\begin{aligned}\frac{d^2\sigma^{(N)}}{dx_b dx_t} &= \frac{4\pi\alpha^2}{9q^2} 4 \int d^3r \sum_f e_f^2 \left[ q_{f,p}(x_b(\vec{r})) \int \frac{d^3p}{(2\pi)^3} \frac{M_N}{E(\vec{p})} \int_{-\infty}^{\mu} dp^0 S_h(p^0, \mathbf{p}) \bar{q}_{f,N}(x'_t) \right. \\ &\quad \left. + \bar{q}_{f,p}(x_b(\vec{r})) \int \frac{d^3p}{(2\pi)^3} \frac{M_N}{E(\vec{p})} \int_{-\infty}^{\mu} dp^0 S_h(p^0, \mathbf{p}) q_{f,N}(x'_t) \right] \theta(x'_t) \theta(1-x'_t) \theta(1-x_b(\vec{r}))\end{aligned}\quad (29)$$

where  $S_h(p^0, \mathbf{p})$  is the hole spectral function for the nucleon in the nucleus.  $q_{f,N} = \frac{1}{2}(q_{f,p} + q_{f,n})$  and  $\bar{q}_{f,N} = \frac{1}{2}(\bar{q}_{f,p} + \bar{q}_{f,n})$  are the nucleon PDFs of flavor  $f$  averaged over quark and antiquark PDFs in proton and neutron. The pion and rho cloud contributions are written as [21]:

$$\begin{aligned}\frac{d^2\sigma^{(\pi)}}{dx_b dx_t} &= \frac{4\pi\alpha^2}{9q^2} (-6) \int d^3r \sum_f e_f^2 \left[ q_{f,p}(x_b(\vec{r})) \int \frac{d^4p}{(2\pi)^4} \theta(p^0) \delta Im D_\pi(q) 2M_N \bar{q}_{f,\pi}(x_\pi) \right. \\ &\quad \left. + \bar{q}_{f,p}(x_b(\vec{r})) \int \frac{d^4p}{(2\pi)^4} \theta(p^0) \delta Im D_\pi(q) 2M_N q_{f,\pi}(x_\pi) \right] \theta(x_\pi - x_t) \theta(1-x_\pi) \theta(1-x_b(\vec{r}))\end{aligned}\quad (30)$$

and

$$\begin{aligned}\frac{d^2\sigma^{(\rho)}}{dx_b dx_t} &= \frac{4\pi\alpha^2}{9q^2} (-12) \int d^3r \sum_f e_f^2 \left[ q_{f,p}(x_b(\vec{r})) \int \frac{d^4p}{(2\pi)^4} \theta(p^0) \delta Im D_\rho(q) 2M_N \bar{q}_{f,\rho}(x_\rho) \right. \\ &\quad \left. + \bar{q}_{f,p}(x_b(\vec{r})) \int \frac{d^4p}{(2\pi)^4} \theta(p^0) \delta Im D_\rho(q) 2M_N q_{f,\rho}(x_\rho) \right] \theta(x_\rho - x_t) \theta(1-x_\rho) \theta(1-x_b(\vec{r}))\end{aligned}\quad (31)$$

Using Jacobian transformation Eq. 29 may be written as:

$$\begin{aligned}\frac{d^2\sigma}{dx_b dM} &= \frac{8\pi\alpha^2}{9M} \frac{1}{x_b s_N} 4 \int d^3r \sum_f e_f^2 \left[ q_{f,p}(x_b(\vec{r})) \int \frac{d^3p}{(2\pi)^3} \frac{M_N}{E(\vec{p})} \int_{-\infty}^{\mu} dp^0 S_h(p^0, \mathbf{p}) \bar{q}_{f,N}(x'_t) \right. \\ &\quad \left. + \bar{q}_{f,p}(x_b(\vec{r})) \int \frac{d^3p}{(2\pi)^3} \frac{M_N}{E(\vec{p})} \int_{-\infty}^{\mu} dp^0 S_h(p^0, \mathbf{p}) q_{f,N}(x'_t) \right] \theta(x'_t) \theta(1-x'_t) \theta(1-x_b(\vec{r}))\end{aligned}\quad (32)$$

To evaluate proton-deuteron Drell-Yan cross section, we write

$$\frac{d\sigma^{pd}}{dx_b dx_t} = \frac{d\sigma^{pp}}{dx_b dx_t} + \frac{d\sigma^{pn}}{dx_b dx_t}. \quad (33)$$

To take into account the deuteron effect, the quark/antiquark distribution function inside the deuteron target have been calculated using the same formula as for the nuclear structure function but performing the convolution with the deuteron wave function squared instead of using the spectral function with the Paris N-N potential.

In terms of the deuteron wave function, one may write

$$q_f^t(x_t, Q^2) = \int \frac{d^3p}{(2\pi)^3} |\Psi_D(\mathbf{p})|^2 q_f^N(x'_t(\mathbf{p}), Q^2) \quad (34)$$

and similar expression for the antiquarks.

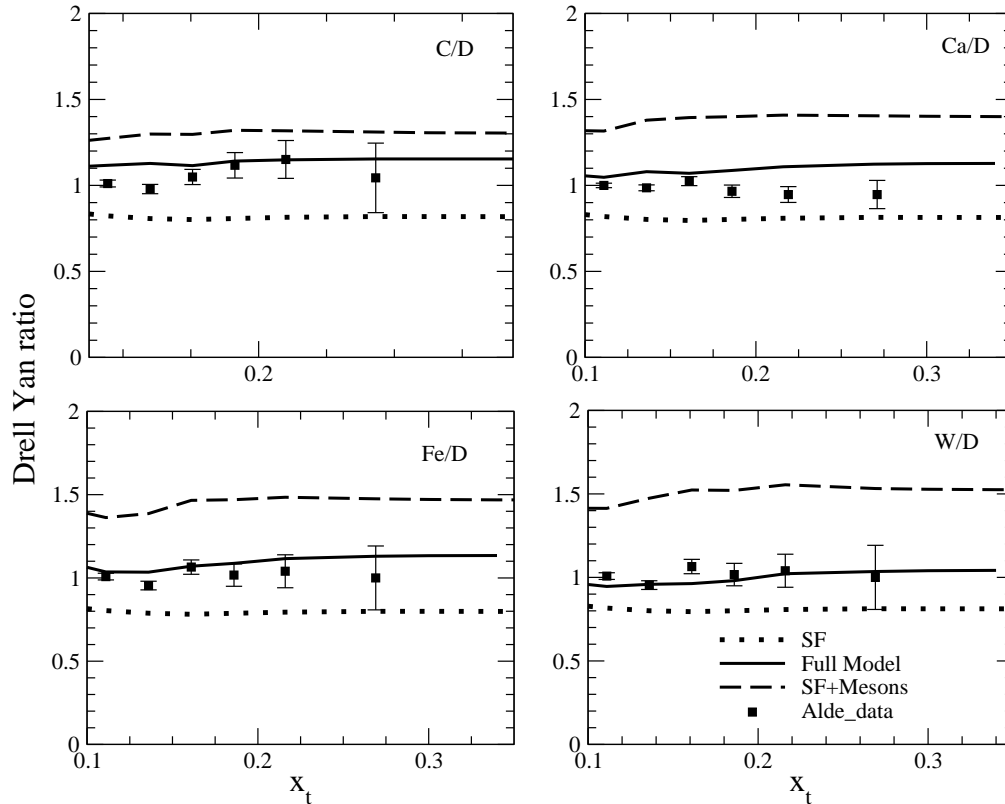


FIG. 1: Left panel:  $\frac{d\sigma}{dx_t}(C,Fe)}{\frac{d\sigma}{dx_t}(D)}$  vs  $x_t$  at  $\sqrt{s_N}=38.8\text{GeV}$ . Spectral function without energy loss: dotted line, spectral function+meson cloud contributions without energy loss:dashed line and the solid line: results with the full model i.e. spectral function+meson cloud contributions with energy loss. For the energy loss we have taken  $\beta = 0.04$ . Experimental points are of E772 experiment [33]. Right panel:  $\frac{d\sigma}{dx_t}(Ca,W)}{\frac{d\sigma}{dx_t}(D)}$  vs  $x_t$ , lines have same meaning as in the left panel.

### III. RESULTS AND DISCUSSION

The numerical results for  $\left(\frac{d\sigma}{dx_t}\right)^A$  for a nucleus A have been evaluated after integrating  $\left(\frac{d\sigma}{dx_b dx_t}\right)^A = \left(\left(\frac{d\sigma}{dx_b dx_t}\right)^N + \left(\frac{d\sigma}{dx_b dx_t}\right)^\pi + \left(\frac{d\sigma}{dx_b dx_t}\right)^\rho\right)$  over  $x_b$  from  $x_b = x_t + 0.26$  to  $x_b = 1$  for  $Q^2 > 16\text{GeV}^2$ . The cross sections  $\left(\frac{d\sigma}{dx_b dx_t}\right)^{i=N,\pi,\rho}$  are evaluated using Eqns.29, 30 and 31 respectively, where the nucleon quark(antiquark) PDFs given by CTEQ6.6 [38] and pion quark(antiquark) PDFs given by Gluck et al. [39] have been used. The spectral function  $S_h(p^0, \mathbf{p})$  with parameters fixed by Eqns.(9), (10) has been used to calculate the nucleon contribution which reproduce the binding energy per nucleon given in Eq. 13 and has no free parameter. For evaluating the mesonic contributions Eqns.(30) and (31) have been used with the parameters of  $D_\pi$  and  $D_\rho$  fixed so that the experimental data on  $F_2^i(x_t)$  for various nuclei  $i=^9\text{Be}$ ,  $^{12}\text{C}$ ,  $^{40}\text{Ca}$  and  $^{56}\text{Fe}$  are reproduced satisfactorily [29]. Taking the energy loss parameter  $\beta$  in Eq.(28) as a variable parameter, we present our results in Fig. 1 for  $\left(\frac{d\sigma}{dx_t}\right)^i$  using  $\beta = 0.04$  and compare them with the experimental results of E772 [33] for  $i=^{12}\text{C}$ ,  $^{40}\text{Ca}$ ,  $^{56}\text{Fe}$ , and  $^{184}\text{W}$  nuclei. In the numerical evaluation of the denominator  $\left(\frac{d\sigma}{dx_t}\right)^D$  i.e. Drell-Yan cross section for the proton-deuteron scattering, we have obtained the results by using Eq. 33 and Eq. 34 (with and without the deuteron effect), where Eq. 34 takes care of deuteron effect. We find the deuteron effect to be small on the ratio R (about 2%) and have not been shown in this figure. We find that the nuclear structure effects due to bound nucleon lead to a suppression in the DY yield of about 16–18% in the region of  $0.1 < x_t < 0.3$  which is larger than what has been found in the case of  $F_2(x_t)$  [29]. On the other hand, there is significant contribution of mesons which increases the DY ratio and overestimates the DY yields which increases with A. For example, in the case of  $^{12}\text{C}$  it is around 18%, 25% in  $^{40}\text{Ca}$ , 35% in  $^{56}\text{Fe}$  and 45% in  $^{184}\text{W}$

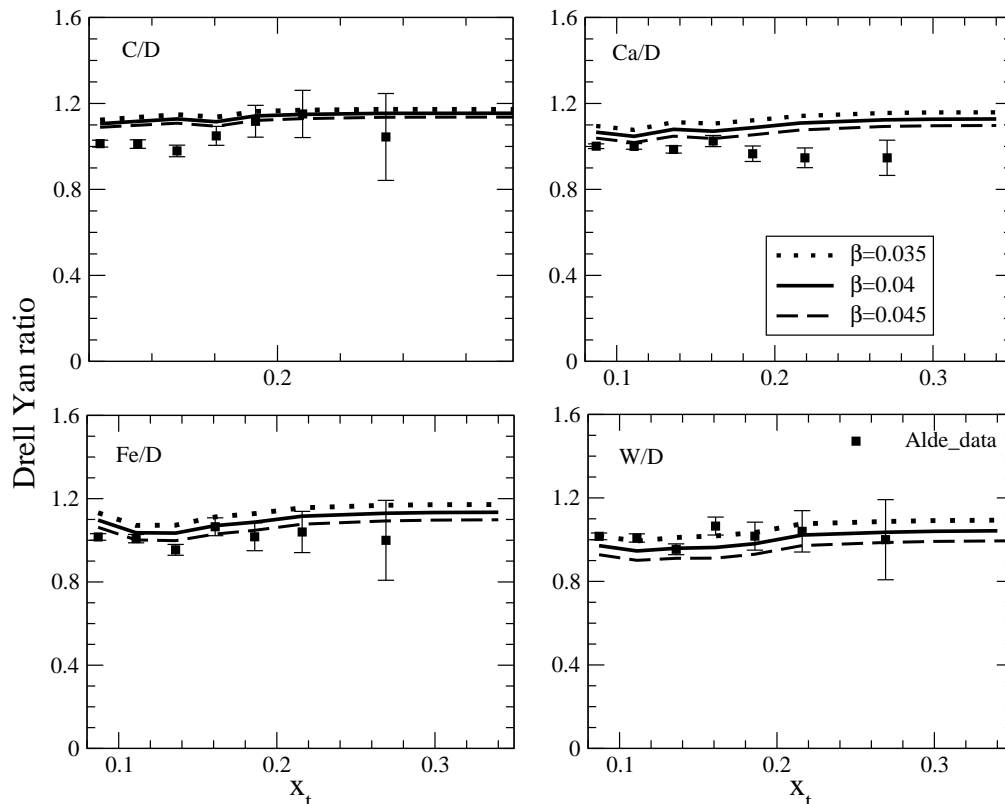


FIG. 2:  $\frac{\frac{d\sigma}{dx_t}(i)}{\frac{d\sigma}{dx_t}(D)}$  vs  $x_t$  at  $\sqrt{s_N}=38.8\text{GeV}$  for  $\beta = 0.04$ .  $i$  stands for the various nuclei like C, Ca, Fe and W. Results are shown for the full model(spectral function+meson cloud contribution) with different values of  $\beta$ , a parameter used in the expression of the energy loss. Experimental points are of E772 experiment [33].

in this range of  $x_t$ . This increase in the DY yield from meson cloud contribution increases with  $A$ . Thus, the mesonic contribution found in the case of DY yields is larger than found in the case of  $F_2(x_t)$  for the nuclei studied here and in Ref. [29]. This contribution is also found to be sensitive to the parameters used in the meson propagators  $D_\pi(p)$  and  $D_\rho(p)$ , but we have used the same parameters which satisfactorily produce the results for the electromagnetic structure function  $F_2(x)$  for all the nuclei like  ${}^9\text{Be}$ ,  ${}^{12}\text{C}$ ,  ${}^{40}\text{Ca}$  and  ${}^{56}\text{Fe}$  and do not treat them as free parameters. We find the contribution from rho meson cloud to be much smaller than the contribution from pion cloud. When we include the energy loss effect, we find that there is a suppression in the DY yield which further decreases with the increase in mass number  $A$ . For example, in the case of  ${}^{12}\text{C}$  it is around 12%, 20% in  ${}^{40}\text{Ca}$ , 25% in  ${}^{56}\text{Fe}$ , and 35% in  ${}^{184}\text{W}$ . The increase in DY yield due to mesonic contribution and suppression due to beam energy loss compensate each other and we get a reasonable agreement with the experimental results for  $\beta = 0.04$ . However, the numerical value of beta needed to reproduce the experimental results can vary depending upon the value of parameter  $\Lambda_\pi$  or  $\Lambda_\rho$  used for evaluating the propagators  $D_\pi$  and  $D_\rho$  in Eqns. 17 and 25. A smaller value of beta ( $< 0.04$ ) would also reproduce the experimental results provided a smaller value of parameter  $\Lambda$  ( $< 1\text{GeV}$ ) is used to evaluate  $D_\pi$  and  $D_\rho$ . In Fig. 2, we show the dependence of DY yield ratio on the energy loss parameter  $\beta$  for  $\Lambda = 1\text{GeV}$ .

In Fig.3, we present our results for  $\frac{\left(\frac{d\sigma}{dx_t}\right)^{Fe}}{\left(\frac{d\sigma}{dx_t}\right)^D}$ , with  $x_b = x_t + 0.26$ , and compare the results with the results of various theoretical calculations available in the literature [13–16, 19, 33]. Our results are presented for the full model with  $\beta = 0.04$ . We see from Fig.3, that our results agree with the results of Close et al. [11], Berger et al. [13] and Jung and Miller [14].

In E866 experiment [26, 34] the results are also presented for  $\frac{d\sigma}{dx_F}$  vs  $x_F$ , where  $x_F = x_b - x_t$  and  $\frac{d\sigma}{dM}$  vs  $M$ , where  $M(= \sqrt{x_b x_t s_N})$ . Using Eqns.29 and 32 we have obtained the results respectively for  $\frac{d\sigma}{dx_F}$  vs  $x_F$  and  $\frac{d\sigma}{dM}$  vs  $M$  and shown these results in Fig.4. For  $\frac{d\sigma}{dx_F}$  vs  $x_F$ , we have integrated over  $x_b$  between the limits  $0.21 \leq x_b \leq 0.95$  and following the kinematical cuts of  $4.0 < M < 8.4$  GeV used in E866 [26, 34] experiment. In the case of  $\frac{d\sigma}{dM}$  vs  $M$ , we have integrated over  $x_b$  between the limits  $0.21 \leq x_b \leq 0.95$  and put the kinematical constraint  $0.13 \leq x_F \leq 0.93$  as



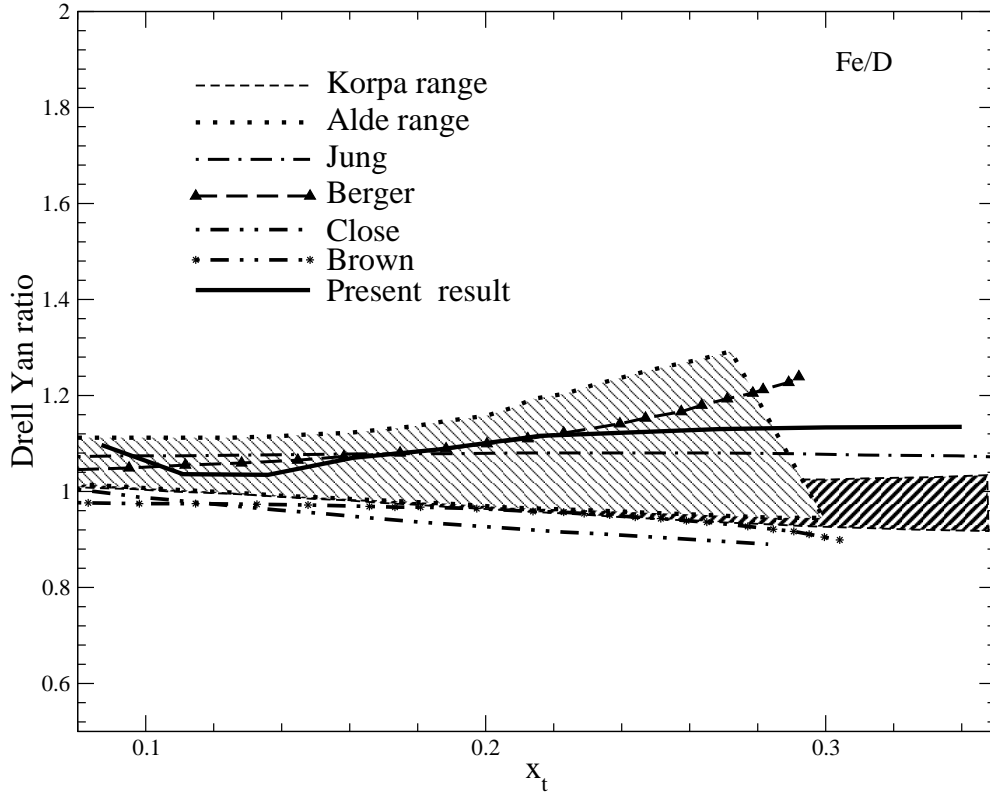


FIG. 3:  $\frac{d\sigma}{dx_t}(Fe)$  vs  $x_t$  at  $\sqrt{s_N}=38.8$  GeV. These results are shown for  $\beta = 0.04$ . Theoretical results of Korpa et al. [19] using different parameter values and Alde et al. [33] in the different models are shown through bands. Dashed line with triangle up: Berger and Coester [13] results, dotted dashed line: Jung and Miller [14] results, double dotted dashed line: results of Close et al. [15] and Double dotted with stars: results of Brown et al. [16]. Solid line is our result with spectral function and meson cloud contributions.

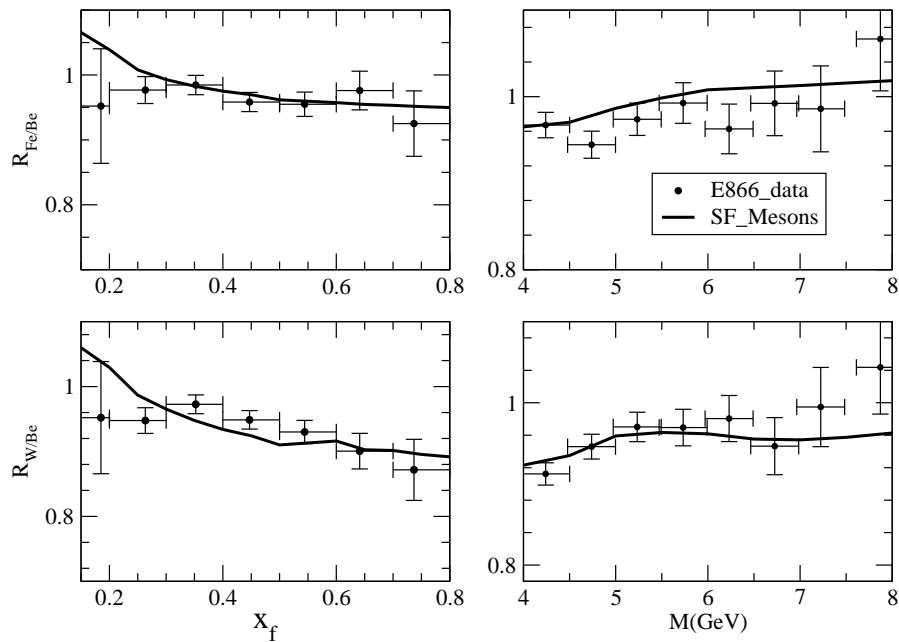


FIG. 4: Left Panel:  $\frac{d\sigma}{dx_F}(Fe,W)$  vs  $x_F$  for  $\beta = 0.04$ , Right Panel:  $\frac{d\sigma}{dM}(Fe,W)$  vs  $M(= \sqrt{x_b x_t s_N})$  GeV, at  $\sqrt{s_N}=38.8$  GeV. Experimental points are of E866 experiment [26, 34]. Spectral Function+Meson cloud contribution: solid line.

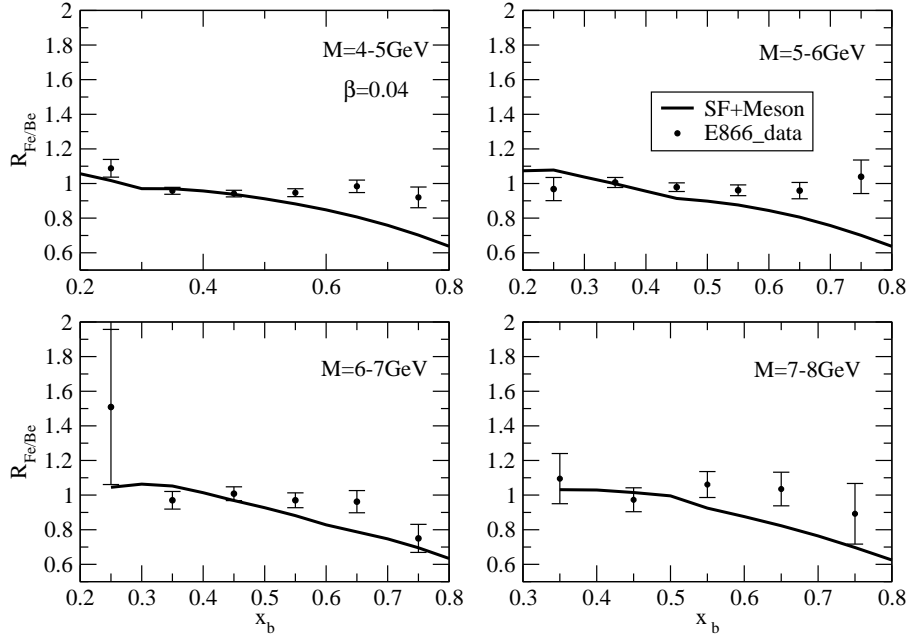


FIG. 5:  $\frac{\frac{d\sigma}{dM dx_b}(Fe)}{\frac{d\sigma}{dM dx_b}(Be)}$  vs  $x_b$  at different  $M(= \sqrt{x_b x_t s_N})$  with  $\sqrt{s_N}=38.8\text{GeV}$ . Experimental points are of E866 experiment [26, 34]. Spectral Function+Meson cloud contribution: solid line.

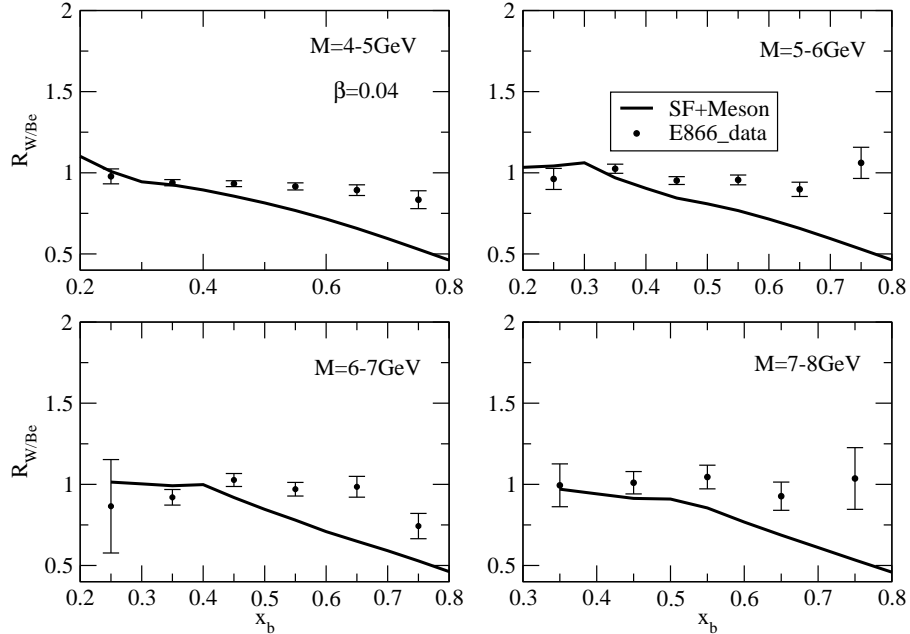


FIG. 6:  $\frac{\frac{d\sigma}{dM dx_b}(W)}{\frac{d\sigma}{dM dx_b}(Be)}$  vs  $x_b$  at different  $M(= \sqrt{x_b x_t s_N})$  with  $\sqrt{s_N}=38.8\text{GeV}$ . Experimental points are of E866 experiment [26, 34]. Spectral Function+Meson cloud contribution: solid line.

used in E866 [26, 34] experiment. These results are shown for the Drell-Yan ratio for  $\frac{(\frac{d\sigma}{dx_F})^i}{(\frac{d\sigma}{dx_F})_{Be}}$  vs  $x_F$  (Left panel) and  $\frac{(\frac{d\sigma}{dM})^i}{(\frac{d\sigma}{dM})_{Be}}$  vs  $M$  (Right panel),  $i$  stands for the iron nucleus (top panel) and tungsten nucleus (bottom panel). We find a good agreement with the experimental results for the various Drell-Yan ratios available from E866 [26, 34] experiment.

In Fig. 5, we present the results for the Drell-Yan ratio for  $\frac{\left(\frac{d^2\sigma}{dx_b dM}\right)^{Fe}}{\left(\frac{d^2\sigma}{dx_b dM}\right)^{Be}}$  vs  $x_b$ (Left panel) for different values of  $M(= \sqrt{x_b x_t s_N})$ , between the same kinematic limits as taken in the numerical evaluation of the results for Fig.4. The results for this ratio for tungsten to beryllium target are shown in Fig. 6.

Keeping the SeaQuest[35] experiment at Fermi Lab in mind where various nuclear targets like deuterium, carbon, iron and tungsten are proposed to be used using a beam energy of 120GeV, in Fig. 7, we present the results for the Drell-Yan ratio for  $\frac{\left(\frac{d^2\sigma}{dx_b dx_t}\right)^i}{\left(\frac{d^2\sigma}{dx_b dx_t}\right)^D}$  vs  $x_b$  for different values of  $x_t$ , for  $Q^2 > 5GeV^2$  at  $E_{Lab} = 120GeV$ ,  $i$  stands for C, Fe and W nuclei.

#### IV. SUMMARY AND CONCLUSION

We have studied nuclear medium effects in Drell-Yan processes at small target  $x_t$  away from the shadowing region( $x_t \geq 0.1$ ) using quark parton distribution functions and nucleon structure functions for a bound nucleon. We have used a microscopic nuclear model which takes into account the effect of Fermi motion, nuclear binding and nucleon correlations through a relativistic spectral function of bound nucleon. The contributions of  $\pi$  and  $\rho$  mesons are also included. We also include the beam energy loss effect due to initial state interactions of protons visualized through inelastic collisions of protons with nuclear constituents before they suffer hard collisions to produce lepton pair. We find a reduction in the DY yield due to nuclear structure effects and an enhancement due to mesonic contribution. Both the reduction as well as the enhancement in the case of DY yields are found to be larger than found in the case of DIS of charged leptons for the same value of model parameters. In the case of DY yields there is a further reduction due to beam energy loss effect in the nuclear medium which has been treated using a parameter describing the beam energy loss. The numerical results are compared with various theoretical results available in the literature and also with the experimental results from E772 [33] and E866 [26, 34] experiments. We find a reasonable agreement with the experimental results presently available for  $^{12}C$ ,  $^{40}Ca$ ,  $^{56}Fe$ , and  $^{184}W$  by suitably varying the beam energy loss parameter. We have also presented in this paper, results for  $\frac{d^2\sigma}{dx_b dx_t}$  vs  $x_b$  for various values of  $x_t$  and the results for  $\frac{d\sigma}{dx_t}$  vs  $x_t$  relevant to the forthcoming E906 SeaQuest [35] experiment at Fermi Lab. Our results show that the model for describing the nuclear medium effects in the DIS of charged leptons and neutrino and antineutrino with nuclear targets is able to explain the experimental results in the case of Drell-Yan yield in the region  $0.1 < x_t < 0.35$  provided a reasonable model for beam energy loss effect is used. High statistics, high precision data from E906 SeaQuest [35] experiment on  $\frac{d^2\sigma}{dx_b dx_t}$  in various regions of  $x_b$  and  $x_t$  will provide important information about the modification of quark PDFs and nucleon structure function in the nuclear medium.

#### V. ACKNOWLEDGEMENTS

M. S. A. is thankful to Department of Science and Technology(DST), Government of India for providing financial assistance under Grant No. SR/S2/HEP-18/2012. I. R. S. thanks FIS2011-24149 Spanish project for financial support.

- 
- [1] S. D. Drell and Tung-Mow Yan, Phys. Rev. Lett. **25**, 316 (1970), Erratum-ibid. **25**, 902 (1970).
  - [2] Deep Inelastic Scattering, Robin Devenish and Amanda Cooper-Sarkar, Oxford University Press, New York 2004.
  - [3] I. R. Kenyon, Rep. Prog. Phys. **45**, 1261 (1982).
  - [4] D. F. Geesaman, K. Saito and A. W. Thomas, Ann. Rev. Nucl. Part. Sci. **45**, 337 (1995).
  - [5] K. J. Eskola, H. Paukkunen, C. A. Salgado, JHEP **0904** (2009), 065; K. J. Eskola, V. J. Kolhinen, H. Paukkunen and C. A. Salgado, JHEP **0705**, 002 (2007), S. Kumano, Phys. Rev. D **43**, 59 (1991); **43**, 3067 (1991), M. Hirai, S. Kumano and T. -H. Nagai, Phys. Rev. C **76**, 065207 (2007), M. Hirai, S. Kumano and T. -H. Nagai, Phys. Rev. C **70**, 044905 (2004).
  - [6] I. Schienbein, J.Y. Yu, C. Keppel, J.G. Morfin, F. Olness and J.F. Owens, Phys. Rev. D **77**, 054013 (2008), I. Schienbein, J.Y. Yu, K. Kovarik, C. Keppel, J.G. Morfin, F. Olness, J.F. Owens, Phys. Rev. D **80** 094004 (2009).
  - [7] R. P. Bickerstaff, M. C. Birse, and G. A. Miller, Phys. Rev. Lett. **53**, 2532 (1984).
  - [8] S. A. Kulagin and R. Petti Phys. Rev. C **82**, 054614 (2010); ibid Phys. Rev. D **76**, 094023 (2007).
  - [9] C. H. Llewellyn Smith, Phys. Lett. B **128**, 107 (1983).
  - [10] C. E. Carlson and T. J. Havens Phys. Rev. Lett. **51**, 261 (1983).
  - [11] F. E. Close, R. G. Roberts and G. G. Ross, Phys. Lett. B **129**, 346 (1983).

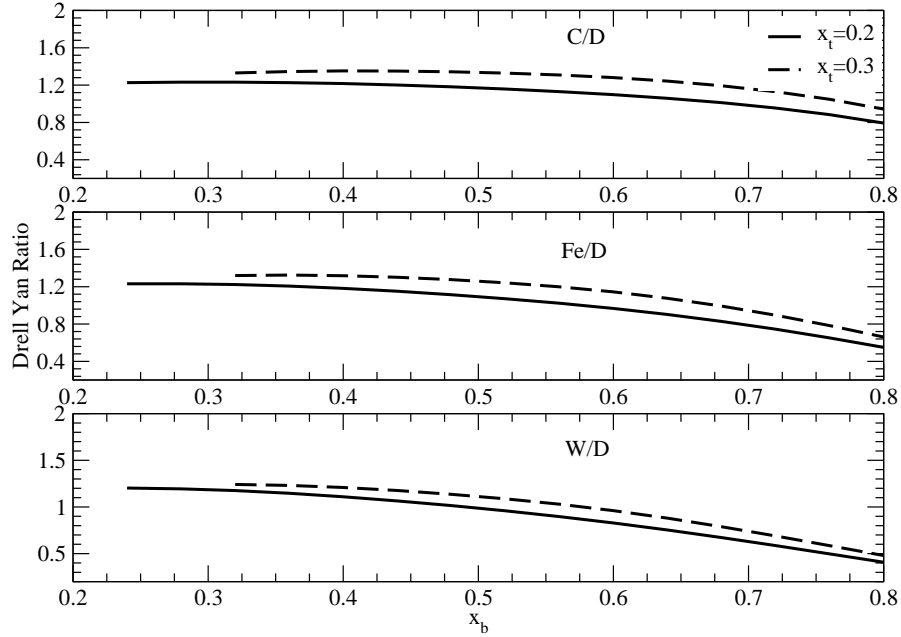


FIG. 7:  $\left(\frac{d^2\sigma}{dx_b dx_t}\right)^i$  vs  $x_b$  at different  $x_t$  for  $E_{Lab} = 120 GeV$ ,  $Q^2 > 5 GeV^2$  and  $\beta = 0.04$ .  $i$  stands for C, Fe and W nuclei.

- [12] M. Ericson and A. W. Thomas, Phys. Lett. B **148**, 191 (1984).
- [13] E. L. Berger and F. Coester, Phys. Rev. D **32**, 1071 (1985).
- [14] H. Jung and G. A. Miller, Phys. Rev. C **41**, 659 (1990).
- [15] F. E. Close, R. L. Jaffe, R. G. Roberts and G. G. Ross, Phys. Rev. D **31**, 1004 (1985).
- [16] G. E. Brown, M. Buballa, Z. B. Li and J. Wambach, Nucl. Phys. A **593**, 295 (1995).
- [17] E. L. Berger, F. Coester and R. B. Wiringa, Phys. Rev. D **29**, 398 (1984).
- [18] R. L. Jaffe and X. -D. Ji, Phys. Rev. Lett. **67**, 552 (1991).
- [19] A. E. L. Dieperink and C. L. Korpa, Phys. Rev. C **55**, 2665 (1997).
- [20] C. L. Korpa and A. E. L. Dieperink, Phys. Rev. C **87**, 014616 (2013).
- [21] E. Marco and E. Oset, Nucl. Phys. A **645**, 303 (1999).
- [22] C.-G. Duan, L.-H. Song, S.-H. Wang, G.-L. Li Eur. Phys. J. C **39** (2005) 179.
- [23] M. B. Johnson et al., Phys. Rev. C **65**, (2002) 025203.
- [24] G. T. Garvey and J. C. Peng, Phys. Rev. Lett. **90** (2003) 092302.
- [25] S. J. Brodsky and P. Hoyer, Phys. Lett. B **298**, 165 (1993).
- [26] M. A. Vasiliev et al., Phys. Rev. Lett. **83**, 2304 (1999).
- [27] E. Marco, E. Oset, and P. Fernandez de Cordoba, Nucl. Phys. A **611**, 484 (1996).
- [28] M. Sajjad Athar, S.K. Singh and M.J. Vicente Vacas Phys. Lett. B **668**, 133 (2008).
- [29] M. Sajjad Athar, I. Ruiz Simo and M. J. Vicente Vacas, Nucl. Phys. A **857**, 29 (2011).
- [30] H. Haider, I. Ruiz Simo, M. Sajjad Athar and M. J. Vicente Vacas, Phys. Rev. C **84**, 054610 (2011).
- [31] H. Haider, I. Ruiz Simo and M. Sajjad Athar, Phys. Rev. C **85**, 055201 (2012).
- [32] H. Haider, I. Ruiz Simo and M. Sajjad Athar, Phys. Rev. C **87**, 035502 (2013).
- [33] D. M. Alde et al., Phys. Rev. Lett. **64**, 2479 (1990).
- [34] E. A. Hawker et al. (FNAL E866/NuSea), Phys. Rev. Lett. **80**, 3715 (1998).
- [35] P. E. Reimer (Fermilab SeaQuest Collaboration), J. Phys.: Conf. Ser. **295**, 012011 (2011).
- [36] P. Fernandez de Cordoba and E. Oset, Phys. Rev. C **46**, 1697 (1992).
- [37] L. L. Frankfurt and M. Strikman Phys. Lett.B **183** 1987 254.
- [38] Pavel M. Nadolsky et al., Phys. Rev. D **78**, 013004 (2008); <http://hep.pa.msu.edu/cteq/public>
- [39] M. Gluck, E. Reya and A. Vogt, Z. Phys. C **53**, 651 (1992).
- [40] J. Beringer *et al.* [Particle Data Group Collaboration], Phys. Rev. D **86**, 010001 (2012).